Effect of ZnO Nanostructures on 2-Dimensional Random Lasing Properties

Xiang Liu, Alexey Yamilov, Xiaohua Wu, Jian-Guo Zheng, Hui Cao, and R. P. H. Chang*

Materials Research Center, Northwestern University, Evanston, Illinois 60208

Received December 19, 2003. Revised Manuscript Received July 19, 2004

We show results on how the morphology of a ZnO layer can have a big impact on the random lasing threshold of the material. Plasma-enhanced chemical vapor deposition method is used to grow ZnO layers on sapphire substrates. The morphologies and structures of ZnO are observed to undergo transition when growth temperature decreases from 750 to 100 °C: the deposited ZnO changes from crystalline films to nanocrystalline films with columnar-shaped grains, then to well-aligned ZnO nanorods, and finally to randomly oriented irregular-shaped grains. ZnO nucleation and surface diffusion rates, coalescence between crystal grains, and preferential growth along *c*-axis play important roles in this transition from continuous films to nanorods. Random lasing properties of our ZnO films and nanorods are studied. The scattering ability of ZnO is critical to control the lasing properties. The lowest lasing thresholds are observed for ZnO films grown between 500 and 600 °C when the films have columnar-shaped grains and not at 750 °C when the ZnO layer has a continuous crystalline film. Calculations based on quasi-2D random lasing are consistent with the experimental results of lasing threshold measurements.

Introduction

ZnO is a wide band gap ($E_g = 3.37$ eV) semiconductor material. Recently ZnO has attracted much interest due to its potential applications in optoelectronic devices, such as short-wavelength lasers and ligh-emitting diodes (LEDs). Most of the research has been focused on the growth of ZnO thin films. Molecular beam epitaxy (MBE),[1] pulse laser deposition (PLD),[2] and chemical vapor deposition (CVD)[3] are among the most commonly used techniques for ZnO film preparation. Deposition techniques utilizing plasma have also been investigated.[4,5] ZnO nanorods and nanowires have also received special attention recently due to their unique properties. While the vapor−liquid−solid (VLS) process has been the most popular method for growth of ZnO nanorods or nanowires,[6] other techniques have also been developed. For example, Park et al. have also reported ZnO nanorod growth by metal-organic vapor-phase epitaxy (MOVPE).[7]

ZnO has high exciton binding energy of 60 meV, which is significantly larger than other materials currently used for blue-green light emitting devices, such as ZnSe (22 meV) and GaN (25 meV), therefore ZnO is a promising candidate for making low-threshold exciton lasers. Chen et al. reported optically pumped lasing of ZnO at room temperature.[1] Tang et al. also reported room-temperature lasing of self-assembled ZnO microcrystalline films.[8]

Random lasing is a novel lasing mechanism which is closely related to scattering and localization of light in disordered media.[9,10] Thus, this is a very different lasing mechanism compared to the classical case where a cavity (with mirrors), and a low-loss and high gain medium are required. In random lasers, laser oscillation occurs in the cavities formed by multiple scattering and provides coherent feedback.[11]

Recently, Cao et al. have reported the observation of random lasing at room temperature in ZnO nanocrystalline powders and polycrystalline thin films.[11,12]

Because random lasing is strongly dependent on scattering in the lasing media, one can expect that the lasing properties vary with ZnO layer morphology. However, little work has been done to study the changes of lasing properties of ZnO associated with different

* To whom correspondence should be addressed. E-mail: r-chang@northwestern.edu.

(1) Chen, Y. F.; Bagnall, D. M.; Koh, H. J.; Park, K. T.; Hiraga, K.; Zhu, Z. Q.; Yao, T. *J. Appl. Phys.* **1998**, *84*, 3912.
(2) Vispute, R. D.; Talyansky V.; Trajanovic, Z.; Choopun, S.; Downes, M.; Sharma, R. P.; Woods, M. C.; Lareau, R. T.; Jones, K. A.; Iliadis, A. A. *Appl. Phys. Lett.* **1997**, *70*, 2735.
(3) Bethke, S.; Pan, H.; Wessels, B. W. *Appl. Phys. Lett.* **1988**, *52*, 138.
(4) Robbins, J. J.; Esteban, J.; Fry, C.; Wolden, C. A. *J. Electrochem. Soc.* **2003**, *150*, C693.
(5) Baxter, J. B.; Wu, F.; Aydil, E. S. *Appl. Phys. Lett*. **2003**, *83*, 3797.
(6) Huang, M. H.; Wu, Y. Y.; Feick, H.; Tran, N.; Weber, E.; Yang, P. D. *Adv. Mater*. **2001**, *13*, 113.
(7) Park, W. I.; Kim, D. H.; Jung S. W.; Yi, G.-C. *Appl. Phys. Lett*. **2002**, *22*, 4232.
(8) Tang, Z. K.; Wong, G. K. L.; Yu, P.; Kawasaki, M.; Ohtomo, A.; Koinuma, H.; Segawa, Y. *Appl. Phys. Lett.* **1998**, *72*, 3270.
(9) Wiersma, D. S.; Bartolini, P.; Lagendijk, A.; Righini, R. *Nature* **1997**, *390*, 671.
(10) Lawandy, N. M.; Balachandran, A. M.; Gomes, A. S. L.; Sauvain, E. *Nature* **1994**, *68*, 436.
(11) Cao H.; Zhao, Y. G.; Ho, S. T.; Seelig, E. W.; Wang, Q. H.; Chang, R. P. H. *Phys. Rev. Lett*. **1999**, *82*, 2278.
(12) Cao, H.; Zhao, Y. G.; Liu, X.; Seelig E. W.; Chang, R. P. H. *Appl. Phys. Lett*. **1999**, *75*, 1213.

10.1021/cm0353557 CCC: $27.50
Published on Web 11/11/2004

morphologies. To better understand the mechanism and optimize the media for achieving random lasing, it is important to study the relation between ZnO structures and lasing properties.

In this work, ZnO is deposited by a plasma-enhanced metal-organic chemical vapor deposition (MOCVD) method. We are able to achieve a morphological transition of ZnO from crystalline film to columnar-grained nanocrystalline films, and finally to well-aligned nanorods on sapphire substrates as the growth temperature decreases. The random lasing thresholds of these ZnO samples with different microscopic structures are measured and compared to simulated values obtained from a quasi-2D model.

Experimental Section

ZnO is grown on *c*-plane sapphire substrates by plasma-enhanced MOCVD in a pulsed organometallic beam epitaxy (POMBE) system. The growth apparatus has been described in previous publications.[13] Diethylzinc (DEZn) and oxygen gas are used as precursors for zinc and oxygen, respectively. During deposition, DEZn precursor is kept in a bubbler cooled to −26 °C and transported into the reaction chamber by helium gas flowing at ∼1 standard cubic centimeters per minute (sccm). Oxygen gas is introduced separately into the reaction chamber at a flow rate of 30 sccm. All gas flows are controlled by mass flow meter controllers. A plasma is excited by a 2.45 GHz microwave generator at 1300 W and maintained in the chamber during ZnO deposition. The chamber pressure is set around 3 mTorr. Substrates are mounted on a resistively heated sample holder whose temperature is controlled by an Omega CN-2011 programmable temperature controller. ZnO are deposited on sapphire substrates under different temperatures from 100 to 750 °C. The morphologies of ZnO samples are studied by transmission electron microscopy (TEM) and scanning electron microscopy (SEM) using Hitachi HF-2000 field emission TEM and Hitachi S-4500 field emission SEM, respectively. X-ray diffraction (XRD) is performed in both 2-circle and 4-circle diffractometers with Cu Kα radiation ($\lambda = 1.542$ Å).

Optical property studies including lasing threshold measurements on ZnO films and nanorods are performed with a frequency-tripled Nd:YAG pulsed laser ($\lambda = 355$ nm) at room temperature. The pulse width of the laser output is 20 picoseconds and usually operated at a repetition rate of 10 Hz. The pump light is focused on the sample at normal angle after attenuation. The beam spot diameter is around 20 μm. Emission from the sample is focused into a spectrometer and recorded by a computer in real time. Pump energy can be controlled by moving a variable filter with a gradient layer of metal coating and it is monitored by a power meter through a beam splitter. Typical pump energy used in this work is on the order of 10^{-9} J.

Results

A. Growth of ZnO with Different Morphologies and Structures. A series of ZnO samples are grown by the POMBE system on *c*-plane sapphire substrates at different temperatures while other conditions are fixed. With decreasing growth temperature, these ZnO samples can be divided into four categories according to their morphologies and structures.

1. Crystalline Films Grown at 750 °C. ZnO samples grown on sapphire at very high temperature (∼750 °C) are found to be epitaxial crystalline films. When analyzed by time-of-flight−secondary ion mass spectroscope (ToF−SIMS; Physical Electronics) with a Ga ion source, no detectable impurities are observed. The XRD $\theta-2\theta$ scan result is shown in Figure 1a. Only (000*l*) peaks are present in the scan from ZnO film on *c*-plane sapphire substrate, which indicates that the ZnO film is also *c*-axis oriented. Despite an extraordinarily large lattice mismatch (18%) between ZnO and sapphire, the full width at half-maximum (fwhm) of the XRD ω rocking curve obtained from ZnO (0002) peak is as narrow as 0.1°, which is comparable to or better than thin films grown by other methods. For example, ZnO films grown by halide vapor-phase epitaxy reported by Takahashi et al. have fwhm around 0.2°.[14] This confirms excellent out-of-plane alignment of ZnO crystal. The in-plane mosaic structures of ZnO films are also studied by XRD ϕ scan on $(10\bar{1}3)$ peaks. As displayed in Figure 1b, six peaks are equally separated by 60°, which clearly shows 6-fold symmetry of ZnO about its *c*-axis. The fwhms of these ϕ peaks are around 0.33°. By comparing the ϕ scan of ZnO film with that of sapphire substrates, it can be seen that there is a 30° in-plane rotation between their lattices which is consistent with the epitaxy relation. These XRD data of $\theta-2\theta$ and ϕ scans confirm that the

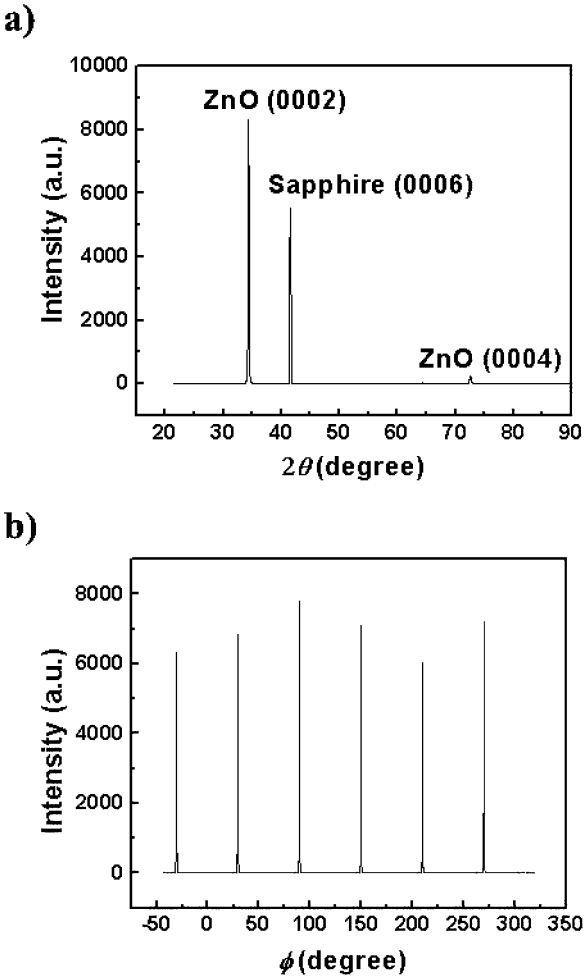

Figure 1. X-ray diffraction (a) $\theta-2\theta$ scan and (b) ϕ scan on ZnO thin films grown on *c*-plane sapphire at 750 °C.

(13) Duray, S. J.; Buchholz, D. B.; Song, S. N.; Richeson, D. S.; Ketterson, J. B.; Marks, T. J.; Chang, R. P. H. *Appl. Phys. Lett.* **1991**, *59*, 1503.

(14) Takahashi, N.; Makino, M.; Nakamura, T.; Yamamoto, H. *Chem. Mater.* **2002**, *14*, 3622.

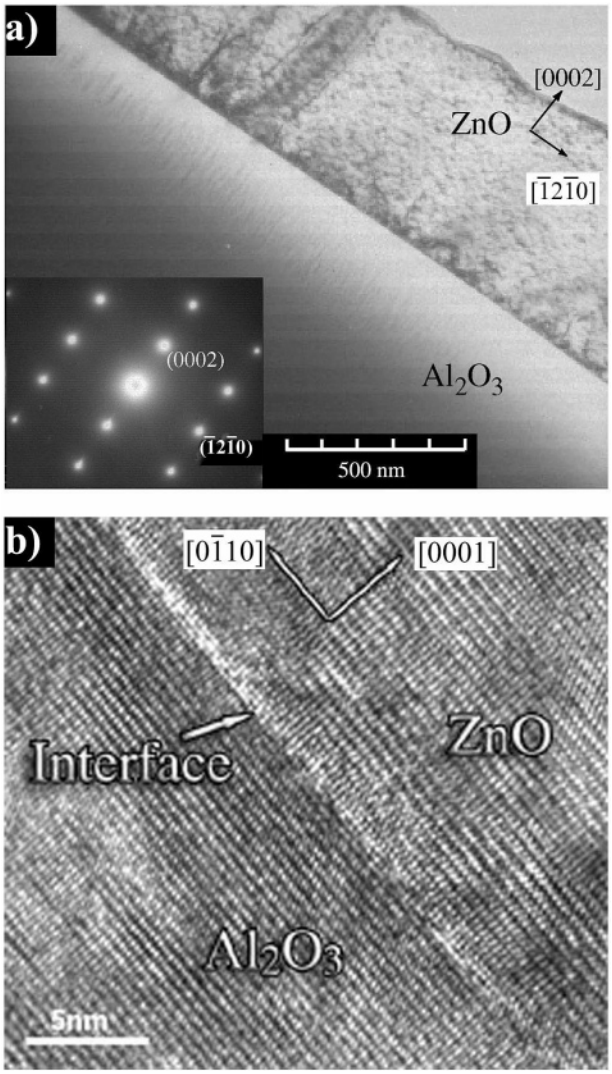

Figure 2. (a) Cross-sectional TEM image of ZnO film grown on sapphire. Inset is selected area electron diffraction pattern taken from ZnO film. (b) High-resolution TEM image at ZnO/Sapphire interface.

ZnO films grown on *c*-plane sapphire at 750 °C have good out-of-plane and in-plane crystal alignments.

Cross-sectional TEM studies are performed on these epitaxial ZnO films. As shown in Figure 2a, no apparent grain boundaries are observed in the cross-sectional TEM image. The selected area electron diffraction (SAED) pattern obtained from the ZnO film is displayed in the inset of Figure 2a. It shows that single-crystal-like ZnO film is grown along the *c*-axis. A high resolution TEM (HRTEM) image taken around the interface area is also shown in Figure 2b. In this image, the interface between film and substrate is clear and abrupt, which implies high-quality epitaxy growth. In areas very close to the interface, misfit dislocations are easily found in the ZnO film; however, the dislocation density decreases rapidly with increasing film thickness. Few dislocations can be found in ZnO film away from the interface region. Therefore, the crystal quality of the ZnO film gets better when the film grows thicker. This improvement of crystallinity with film thickness can also be confirmed by the narrowing of XRD rocking curve peak width as observed in our XRD studies.

On the basis of the above results we can conclude that, at high temperature of 750 °C, high-quality crystalline ZnO films are grown on sapphire substrates in our POMBE system.

2. Columnar-Grained Nanocrystalline Films Grown Between 500 and 700 °C. When the growth temperatures are between 500 and 700 °C, ZnO films grown on sapphire substrates exhibit columnar-shaped nanocrystalline grains. A comparison of ZnO morphologies is shown in the top-view and cross-sectional-view SEM pictures in Figure 3. Films grown between 500 and 700 °C have quite different morphologies compared to those deposited at higher temperatures. As shown in Figure 3a, ZnO films grown at 750 °C are continuous without any apparent grain boundaries in the cross-sectional SEM. However, ZnO films deposited between 500 and 700 °C are composed of columnar grains in close contact with each other. These grains typically have diameters around 100 nm and they are well aligned vertically to the substrate surface (see Figure 3b). XRD data show that these grains are also growing along the *c*-axis of ZnO crystal.

3. Well-Aligned ZnO Nanorods Grown Between 300 and 400 °C. Interestingly, ZnO nanorods are obtained on *c*-plane sapphire at 300 to 400 °C when other growth conditions are kept the same as those for growing ZnO thin films. As shown in Figure 3c and d, needlelike nanorods are densely grown on sapphire substrates. The diameters of the ZnO nanorods are around 50−100 nm, and the length can be as long as several micrometers, depending on the growth time. From top-view SEM images, these ZnO nanorods are uniformly grown on sapphire substrates and they are clearly separated from each other, although the distances between them are quite small. The cross-sectional view SEM picture reveals that these nanorods are very well aligned along the same direction, perpendicular to the substrate surface. XRD results of these samples show that the ZnO nanorods are mostly along the *c*-axis with 0.5−5° deviation.

No metal impurities can be observed in energy dispersive X-ray analysis (EDX) of the ZnO nanorods therefore they are not grown by VLS mechanism.[6] Our growth method is also different from the results reported by Park et al.[7] in which a low-temperature seed layer is deposited before the rod growth begins.

4. ZnO Films With Irregular Grains Grown at 100 °C. If ZnO is grown at very low temperatures, for example at 100 °C, the morphology of the film on *c*-plane sapphire is shown to consist of randomly oriented irregular-shaped grains (Figure 3e) which are different from the columnar grains observed in ZnO films deposited at higher temperatures (as seen in Figure 3b). XRD data show that the crystallinity of the low-temperature film is very poor, the fwhm of ω rocking curve of ZnO (0002) peak is wider than 10°.

B. Lasing Properties of ZnO Films and Nanorods. Random lasing properties of the ZnO films and nanorods are studied. All of the samples have similar thickness around 600−750 nm on *c*-plane sapphire substrates. The lasing threshold is determined by the emergence of discrete sharp spikes in the emission spectra. A typical lasing spectrum of a nanocrystalline ZnO film is shown in Figure 4. The width of a single

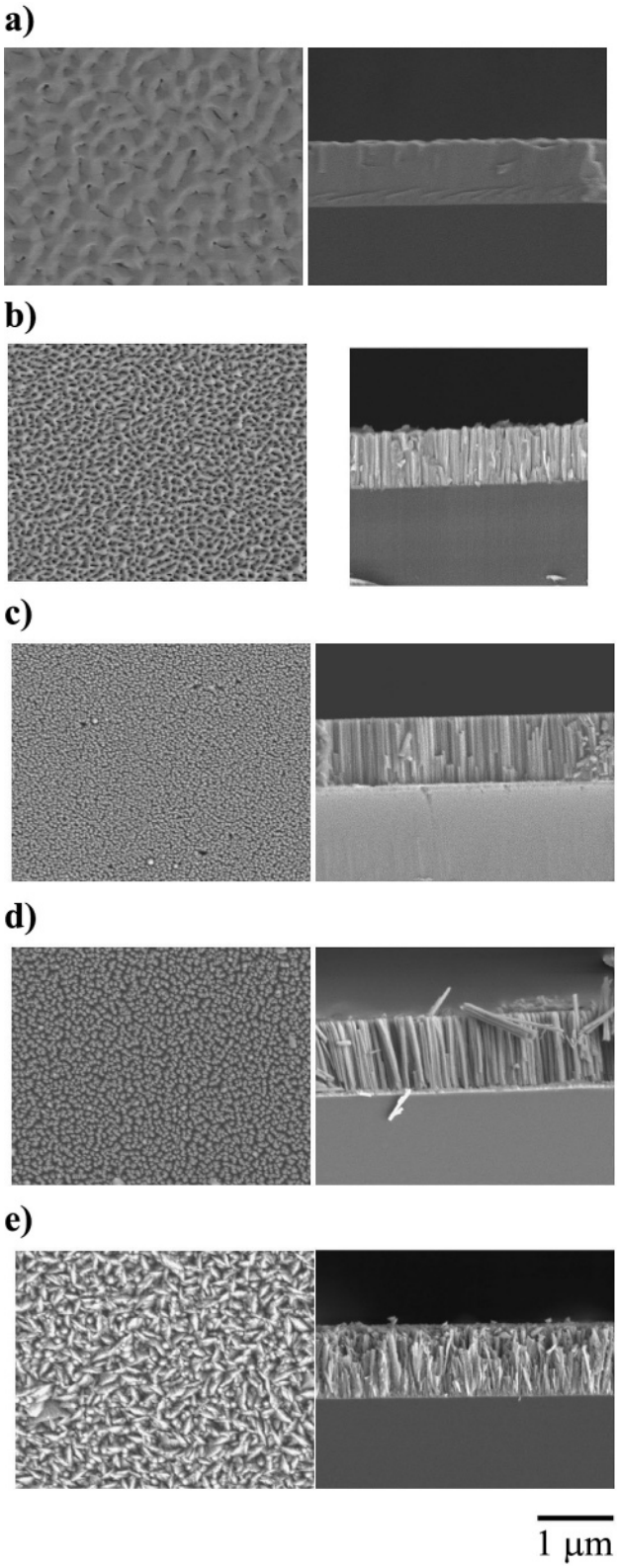

Figure 3. SEM images of ZnO grown on sapphire at (a) 750 °C, (b) 600 °C, (c) 400 °C, (d) 300 °C, and (e) 100 °C (left, top view; right, cross-sectional view).

narrow peak is less than 0.3 nm. Similar random lasing phenomenon observed in ZnO powder and films have been reported by Cao et al.[11]

The relation between lasing threshold and growth temperature of ZnO layers is plotted in Figure 5. The minimum lasing threshold is observed in the ZnO nanocrystalline films deposited at 500−600 °C.

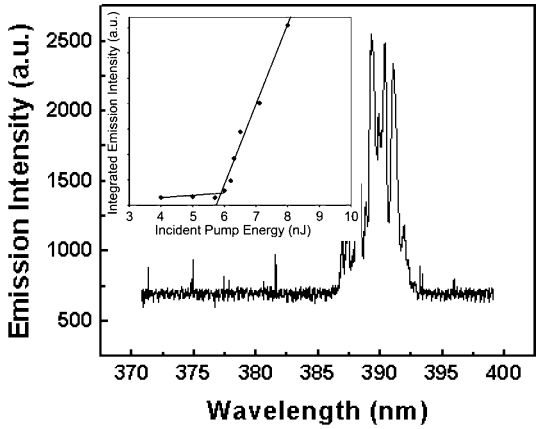

Figure 4. Typical lasing spectrum of a nanocrystalline ZnO film when optically pumped by a frequency-tripled Nd:YAG laser. Inset shows the threshold behavior of the integrated emission intensity with increasing pump energy.

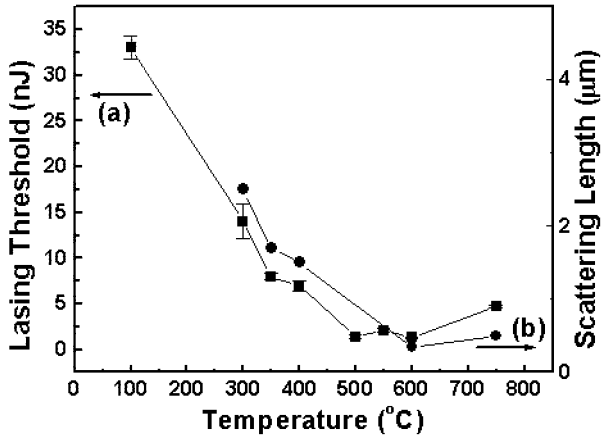

Figure 5. Relations between (a) lasing threshold and growth temperature, and (b) scattering length and growth temperature, of ZnO thin films and nanorods.

Discussion

A. Effect of Growth Temperature on ZnO Morphology. Although studies on the effect of growth conditions on ZnO nanorods or whiskers properties, such as crystallinity and diameter, have been published[15−17] for MOCVD grown ZnO on sapphire, the morphology transition from continuous films to nanorods due to the variation of substrate temperature has not been reported before. While the mechanism of this transition is not fully understood, we think several issues could be relevant to the phenomenon as explained below.

First is the relation between stable nuclei density and substrate temperature. Due to large lattice mismatch between ZnO and sapphire (18%), ZnO forms island-shaped nuclei on the substrate surface at the early stage of CVD deposition. [18,19] In kinetic models of nucleation, the stable nuclei density increases with deposition time at the beginning, then saturates at a certain value

(15) Wu, J.; Liu, S. J. *Phys. Chem. B* **2002**, *106*, 9546.
(16) Wu, J.; Liu, S. J. *Adv. Mater*. **2002**, *14*, 215.
(17) Saitoh, H.; Satoh, M.; Tanaka, N.; Ueda, Y.; Ohshio, S. *Jpn. J. Appl. Phys.* **1999**, *38*, 6873.
(18) Yamauchi, S.; Handa, H.; Nagayama A.; Hariu, T. *Thin Solid Films* **1999**, *345*, 12.
(19) Yamauchi, S.; Ashiga, T.; Nagayama A.; Hariu, T. *J. Cryst. Growth* **2000**, *4/215*, 63.

which depends on deposition rate and temperature. When deposition rate is fixed, the saturated nucleation density can be expressed by the following equation[20] (p. 211 of ref 20):

$$N_s = A \exp(E/kT)$$

where N_S is nucleation density, E is related to activation energy of desorption or surface diffusion, T is growth temperature, and A and k are constants. It is clear that the stable nuclei density decreases with increasing temperature. Second and more importantly is the relation between diffusion and growth temperature: the diffusion coefficient increases with temperature, therefore higher temperature will lead to faster surface diffusion.

On the basis of the above discussion, higher temperature results in lower nuclei density and faster diffusion. It has been well studied that the grain structures of thin films are strongly affected by nucleation and diffusion (reference 20, p 223). In the case of ZnO growth, at 750 °C, the distances between ZnO nuclei are greater on the substrate surface when they are deposited at the beginning of the growth. Facilitated by fast diffusion, ZnO nuclei are allowed to coarsen to reduce the surface area. Small grains will disappear and larger grains will grow at the expense of the smaller ones. When the growth temperature is lowered to between 500 and 700 °C, higher nuclei density and lower diffusivity give rise to smaller and columnar-shaped grains. Although the grains are still in contact to form a nanocrystalline thin film, the amount of boundary areas is obviously much larger as shown in Figure 3c. Between 300 and 400 °C, the lateral growth of ZnO crystal is very limited due to slow diffusion under low temperature. Under these conditions the growth of nanorods is made possible.

Other factors facilitating nanorod growth could include the preferential growth of ZnO along its *c*-axis direction. It has been reported that ZnO crystal grows faster along *c*-axis than other directions. [21] As mentioned earlier, ZnO nanorods in this work are grown along *c*-axis, and the preferential growth rate could have a significant contribution to this alignment.

B. Relation Between Crystallinity and Growth Temperature. The crystallinity of ZnO grown on sapphire by POMBE system is strongly related to the growth temperature. Despite the morphology transition, the crystallinity of ZnO improves with increasing growth temperature. The fwhms of ZnO XRD (0002) ω rocking curve vs growth temperature is plotted in Figure 6. The narrowest XRD peak width, which indicates the best crystallinity, is obtained from ZnO films grown at 750 °C. For ZnO nanorods prepared at 400 °C, the fwhm of the rocking curve peak is around 0.91°. Because of the extremely thin diameters of the nanorods, the effect of finite crystal size on the XRD peak width has to be considered in ω rocking curve scan, which is a transverse scan in the reciprocal space. Thus, the broadening of XRD rocking curves of ZnO nanorods is not solely due to out-of-plane alignment of ZnO crystals. According to the Scherrer equation, for ZnO nanorods which are 50 nm in diameter the XRD rocking curve peak broadening due to finite crystal size can be estimated to be 0.17°. Therefore, the actual out-of-plane misalignment of ZnO nanorods is as small as ~0.7°. This result confirms good crystallinity and vertical-alignment of ZnO nanorods on sapphire substrates.

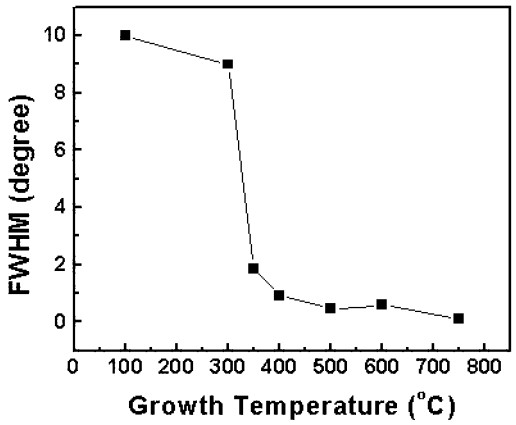

Figure 6. Fwhms of XRD ω rocking curve obtained from ZnO (0002) peak vs growth temperature.

C. Relation between Lasing Properties and ZnO Structures. Random lasing phenomenon has been studied in highly disordered materials including ZnO powders and polycrystalline films.[12] In such structures, ZnO provides optical amplification as a gain media and light forms close loops by multiple scattering. These loops can serve as laser resonators. In this work, high density, well-aligned ZnO nanorods can introduce strong scattering at ZnO−air interfaces while providing optical gain inside each nanorod with good crystallinity. In ZnO thin films, there are sparsely populated microvoids which can cause scattering. In addition, Ong et al. has suggested that grain boundaries are also scattering centers due to refractive index difference at the boundaries and inside the grains.[22] Therefore, both nanorods and nanocrystalline films of ZnO are suitable for random lasing studies.

As shown in Figure 5, random lasing thresholds are quite different for different ZnO structures grown by our POMBE system. The lowest lasing thresholds are obtained from nanocrystalline ZnO thin films deposited between 500 and 600 °C, and ***not*** at the higher temperature, 750 °C. To understand this observation, factors which affect random lasing properties have to be considered. Because random lasing is a result of combination between multiple scattering and light amplification, the lasing properties should be related to the scattering ability and optical gain of the media.

Although quantitative measurements of scattering and gain are not performed in this work, the results can still be explained qualitatively: On one hand, in polycrystalline ZnO film grown at very low temperature, for example at 100 °C, the crystallinity of the film is poor as mentioned in the XRD data. Very high density of crystal defects lead to a large amount of nonradiative recombination which quenches lasing activity in ZnO

(20) Ohring, M. *The Materials Science of Thin Films*, 1st ed.; Academic Press: London, 1992.

(21) Suscavage, M.; Harris, M.; Bliss, D.; Yip, P.; Wang, S. Q.; Schwall, D.; Bouthillette, L.; Bailey, J.; Callahan, M.; Look, D. C.; Reynolds, D. C.; Jones, R. L.; Litton, C. W. *MRS Internet J. Nitride Semiconduct.r Res.* **1999**, *4*, No. G3.40.

(22) Ong, H. C.; Dai, J. Y.; Hung, K. C.; Chan, Y. C.; Chang, R. P. H.; Ho, S. T. *Appl. Phys. Lett.* **2000**, *77*, 1484.

films. So very high pump power is required to achieve lasing in such defective films. On the other hand, in higher quality films grown at 300−750 °C the scattering strength is the determining factor. The detailed analysis made in ref 23 showed the direct relation between the random lasing threshold and the scattering length in the system. Generally, shorter scattering length corresponds to higher scattering abilities and therefore lower lasing threshold in this case. The system studied in this paper is quasi-2D, so one has to pay particular attention to the additional source of leakage in the growth direction. However, for the films grown at 300−750 °C, the filling fraction was sufficiently high (64−91%), so that the effective index of ZnO layer ($n \approx 2.2$) was greater than that of the sapphire ($n \approx 1.79$). The waveguiding effect ensured the confinement in the growth direction. When considering modes guided in a planar layer one usually deals with the modes of two distinct symmetries: transverse magnetic (TM; electric field perpendicular to the plane) and transverse electric (TE; electric field in the plane). Previous polarization measurements[24] of random lasing threshold in systems with film geometry similar to ours showed that the lasing modes have TE structure. To calculate the scattering length for the TE fundamental waveguide mode in 2-D we make the simplest approximation:[23] $l_s = 1/(\rho\sigma)$, where l_s is the scattering length, ρ is the density of scattering units, and σ is the scattering cross section. To estimate the value of ρ for each deposition temperature for ZnO, we make the following assumptions: (i) for samples grown at 300, 350, and 400 °C, we assume the ZnO nanorods to have infinite lengths. We measured the dielectric cylinder diameters to be 34, 37 and 39 nm, respectively. (ii) for samples grown at 600 and 750 °C, the layers are continuous films with sparsely populated microscopic voids. Thus, we can model them as infinite ZnO layers with cylindrical air holes with 80 and 160 nm diameters, respectively. We can estimate the value for ρ based on filling fraction of each ZnO structure observed in SEM: the average separations of elementary scattering units (ZnO cylinders and air holes in above cases) for the five samples with increasing growth temperatures are 41, 42, 43, 200, and 500 nm, respectively. We used the well-known Mie solution[25] to find σ for various cylinder/air-hole radii. For five samples considered above, our calculations yield 2.5, 1.7, 1.5, 0.35, and 0.5 μm scattering length. The obtained l_s values correctly reproduce the behavior of the lasing threshold shown on Figure 5. Thus, the optimal lasing thresholds are expected in ZnO nanocrystalline films deposited between 500 and 600 °C. This result demonstrates the difference between random lasing phenomenon and the classical lasing phenomenon as reported in refs 1 and 8.

Conclusions

ZnO layers are grown on sapphire substrates at different temperatures by plasma-enhanced MOCVD method. A transition of morphology from high-quality epitaxy films to nanocrystalline films, then to well-aligned nanorods, is observed as a function of growth temperature. ZnO nucleation, diffusion, and preferential growth along the *c*-axis play important roles in this interesting transition. The random lasing properties in these ZnO layers are studied and discussed. Films grown at 500 to 600 °C are found to have the lowest lasing thresholds. Calculations based on quasi-2D random lasing in ZnO structure are consistent with the experimental results of lasing threshold measurements

Acknowledgment. This work is supported in part by the MRSEC program of the National Science Foundation (DMR-0076097), National Science Foundation (ECS-0244457), and NASA under award NCC 2-1363. Microscopic work is done in EPIC at Northwestern University.

CM0353557

(23) Wu, X. H.; Yamilov, A.; Noh, H.; Cao, H.; Seelig E. W.; Chang, R. P. H. *J. Opt. Soc. Am. B* **2003**, special issue on Random Lasers, accepted for publication.

(24) Zhao, Y. G.; Cao, H. unpublished data.

(25) Bohren, C. F.; Huffman, D. R. *Absorption and Scattering of Light by Small Particles*; John Wiley and Sons: New York, 1983.